



## Transformation of inert $\text{PbSO}_4$ deposit on the negative electrode of a lead-acid battery into its active state

Bo Zhang<sup>a,b</sup>, Juhua Zhong<sup>b,\*</sup>, Wenjun Li<sup>b</sup>, Zhongyi Dai<sup>b</sup>, Bo Zhang<sup>b</sup>, Zhenmin Cheng<sup>a</sup>

<sup>a</sup> State Key Laboratory of Chemical Engineering, East China University of Science and Technology, 130 Meilong Road, Shanghai 200237, PR China

<sup>b</sup> Department of Physics, East China University of Science and Technology, 130 Meilong Road, Shanghai 200237, PR China

### ARTICLE INFO

#### Article history:

Received 25 August 2009

Received in revised form 4 December 2009

Accepted 20 January 2010

Available online 25 January 2010

#### Keywords:

Lead-acid battery

Lead sulfate

Inverse charging

Battery materials restoring

### ABSTRACT

Different forms of lead sulfate ( $\text{PbSO}_4$ ) are produced in both the cathode and anode in the course of discharging of a lead-acid battery. However, their difference in reaction activity has not been well recognized up to now. From this work, it is shown the cathode product  $\text{PbSO}_4(\text{O})$  due to oxidation of Pb is rather inert and its accumulation could lead to decrease of the battery capacity and life; on the other hand, the anode product  $\text{PbSO}_4(\text{R})$  due to reduction of  $\text{PbO}_2$  has a much active property and is readily reversible in the charging–discharging recycles. To restore the battery capacity, it is critical to solve the deactivation of cathode by transforming  $\text{PbSO}_4(\text{O})$  into  $\text{PbSO}_4(\text{R})$ . For such a purpose, inverse charging is performed, and a procedure from  $\text{PbSO}_4(\text{O})$  to  $\text{PbO}_2$  and to  $\text{PbSO}_4(\text{R})$  is conducted under a series of measurements with cyclic voltammetry, electrochemical impedance spectroscopy, scanning electronic microscopy and X-ray diffraction spectroscopy. The results of inverse charging tests show that the new capacity of a sulfated battery is more than twice of the initial value, which proves the validity of the mechanism outlined.

© 2010 Elsevier B.V. All rights reserved.

## 1. Introduction

Sulfation of the cathode material Pb has been a troublesome problem in lead-acid batteries [1–3]. The sulfation product  $\text{PbSO}_4$  is produced from oxidation of Pb in the charging of the battery, however,  $\text{PbSO}_4$  would deposit on the electrode in the form of fine crystallized particles and is inactive in the charging–discharging recycles according to Catherino et al. [2]. When the lead-acid battery is operated under the condition of a prolonged shortage of capacity or deeply discharged, a large bulk of  $\text{PbSO}_4$  will be formed on the electrode, and the crystallization of  $\text{PbSO}_4$  could result in a more serious situation which makes it difficult to recharge the battery. In the literature, several additives, such as graphite carbon, expanded graphite,  $\text{Al}_2\text{O}_3$ ,  $\text{TiO}_2$ ,  $\text{BaSO}_4$ , etc., have been employed to prevent the sulfate accumulation [4–7]. However, if the negative electrode has already been sulfated, the  $\text{PbSO}_4$  cannot be recovered by using additives. In a different attempt, Stienecker et al. [8] reported that sulfation can be greatly reduced under a current that uses an ultracapacitor in conjunction with the battery for mild hybrid electric vehicles. But, this method cannot be used to recover the sulfated lead-acid batteries applied in other fields. Moreover, pulse or intermittent charging was used to solve the problem of sulfation and premature failure of the negative electrode due to the

high-rate partial state of charge (HRPSoc) operation [9,10]. Nevertheless, the effect of this method to recover the sulfated battery is not significant. Recently, Karami et al. [11,12] have recovered the discarded batteries owing to sulfation by inverse charging, which is reported to be very economic and feasible to operate. Yamamoto et al. [13] recovered the inactive negative electrode by repeating redox process in the positive potential field. However the mechanism of the two methods has not been ascertained.

In this paper, it is suggested for the first time that  $\text{PbSO}_4$  generated from the reduction of  $\text{PbO}_2$ , denoted as  $\text{PbSO}_4(\text{R})$ , and  $\text{PbSO}_4$  from the oxidation of Pb, denoted as  $\text{PbSO}_4(\text{O})$ , have a significant difference in reaction activity. In this consideration, the inverse charging could enable  $\text{PbSO}_4$  on negative electrode to be oxidized to  $\text{PbO}_2$  first, and then reduced to  $\text{PbSO}_4$ . Therefore,  $\text{PbSO}_4(\text{O})$  will be finally transformed into  $\text{PbSO}_4(\text{R})$  and thus constitutes a novel battery recovery procedure.

## 2. Experimental

### 2.1. Electrodes and experimental cell

The electrochemical investigation was performed in a three-electrode system with 4 M  $\text{H}_2\text{SO}_4$ . The working electrode was a pure lead rod (>99.994%) which has an apparent exposed area of about 0.6  $\text{cm}^2$ . A  $\text{Hg}/\text{Hg}_2\text{SO}_4/4\text{M H}_2\text{SO}_4$  electrode was employed as reference electrode. All potentials in this work are presented vs. this reference electrode. The counter electrode was a platinum

\* Corresponding author. Tel.: +86 21 6425 1493; fax: +86 21 6425 2018.  
E-mail addresses: [jhzhong@ecust.edu.cn](mailto:jhzhong@ecust.edu.cn), [phyzjh@126.com](mailto:phyzjh@126.com) (J. Zhong).

foil. Prior to each experiment, the working electrode was polished successively with three grades of abrasive paper, rinsed with anhydrous ethanol (AR), and then washed with doubly distilled water. At last, the electrode was immersed in the electrolyte and subjected to polarization at  $-2.0\text{ V}$  to allow for its surface to be cleaned electrochemically. All the experiments were carried out at room temperature (298 K).

## 2.2. Cyclic-voltammetric (CV) measurements of Pb electrode

CV test was facilitated with an electrochemical working station (CHI 650C) at the potential range from the initial to  $2.0\text{ V}$ , and the scanning rate was fixed at  $50\text{ mV s}^{-1}$ . The initial potential was changed in a large range, and the influence of the initial potential on shapes of the anodic peaks corresponding to the oxidation of  $\text{PbSO}_4$  and the oxygen evolution was investigated.

## 2.3. Preparation of $\text{PbSO}_4(\text{O})$ and $\text{PbSO}_4(\text{R})$ for other characterizations

The samples of  $\text{PbSO}_4(\text{O})$  and  $\text{PbSO}_4(\text{R})$  were prepared by potential stepping method in the three-electrode system. The  $\text{PbSO}_4(\text{O})$  was obtained as follows. Firstly, the lead electrode was held at  $-2.0\text{ V}$  for 600 s, and then the potential was stepped to  $-0.95\text{ V}$ , at which Pb was oxidized to  $\text{PbSO}_4(\text{O})$  [14], and was kept constant for 3600 s. In preparing  $\text{PbSO}_4(\text{R})$ , the lead electrode was firstly held at  $2.0\text{ V}$  for 600 s and  $\text{PbO}_2$  is formed, and then the potential was stepped to  $0.96\text{ V}$  and was kept constant for 3600 s, at which  $\text{PbO}_2$  was reduced to  $\text{PbSO}_4(\text{R})$  [14].

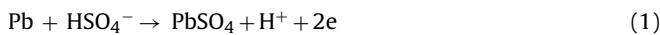
## 2.4. Characterization of the two types of $\text{PbSO}_4$

Two samples of  $\text{PbSO}_4(\text{O})$  and  $\text{PbSO}_4(\text{R})$  with a length about 5 mm were cut-off from the two electrodes for the SEM (scanning electronic microscopy) test. The morphologies of the  $\text{PbSO}_4(\text{O})$  and  $\text{PbSO}_4(\text{R})$  were examined by SEM with JSM-6380. The EIS (electrochemical impedance spectroscopy) experiments of the samples were conducted using an electrochemical working station (CHI 650C) at the range of 10 Hz to 100 kHz and the test results were analyzed by means of ZSimpWin software. The powders of the two samples were scraped off from the two electrodes, and the phase composition was analyzed by X-ray diffractometer (Rigaku D/max-2550) (Cu/ $K\alpha_1$  radiation,  $\lambda = 0.154056\text{ nm}$ ; generator settings: 40 kV, 100 mA).

## 2.5. Mechanism of the inverse charging

Reactions taking place during discharge of a lead-acid battery are described as:

- For the negative electrode or cathode,

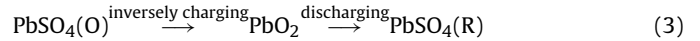


- For the positive electrode or anode,



According to Eqs. (1) and (2),  $\text{PbSO}_4$  are formed both on the cathode from the oxidation of Pb and on the anode from the reduction of  $\text{PbO}_2$ , and are denoted as  $\text{PbSO}_4(\text{O})$  and  $\text{PbSO}_4(\text{R})$  respectively. When the battery is working under deeply discharged or prolonged shortage of capacity, a large number of  $\text{PbSO}_4(\text{O})$  will be formed and crystallized on the negative electrode.

In the suggested process of inverse charging, the following reaction scheme taking place on the negative electrode is outlined:



$\text{PbSO}_4(\text{O})$  on negative electrode is transformed into  $\text{PbSO}_4(\text{R})$ , and the sulfation is resolved.

## 2.6. The inverse charging tests

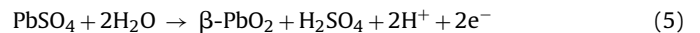
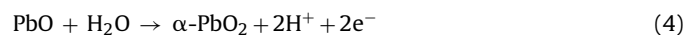
The inverse charging of a sulfated battery was carried out using a DC power supply. Charging and discharging of the battery were performed by a commercial facility (Cycle Charge/Discharge Tester  $\mu\text{C-CF30}$ ). The sulfated battery used in this test was a vented battery with the capacity of 4 Ah and a voltage of 2 V. The battery was first charged at 1.2 A till the voltage reached 2.4 V, and it was then charged at a constant voltage of 2.4 V till the current dropped to 0.2 A. The discharging capacity was measured at a constant discharging current of 1 A (4 h rate) till the voltage decreased to 1.75 V (cut-off voltage). After above steps, the battery was inversely charged at a constant current of 1 A for 14 h and at a constant voltage of 2.6 V for another 12 h. Subsequently, the battery was charged and discharged for one cycle. Finally, the capacities of the battery before and after inverse charging were compared.

## 3. Results and discussion

In order to confirm the differences of the two types of  $\text{PbSO}_4$ , the oxidizing process of  $\text{PbSO}_4$  was studied in the CV measurements, while the morphology, electrochemical reaction activity and the crystal form of the two types of  $\text{PbSO}_4$  were investigated through further SEM, EIS and XRD tests.

### 3.1. CV measurements of Pb electrode

In general, in the cathodic or negative scanning, the  $\text{PbO}_2$  is first reduced to  $\text{PbSO}_4$  from about 1.2 to 0.8 V, and is further reduced to Pb from about  $-1.0$  to  $-2.0\text{ V}$  as reported [14]. On the other hand, Pb can be reduced from  $-0.75$  to  $-0.94\text{ V}$  [15,16]. Therefore, when the initial potential of the scanning is lower than  $-1.0\text{ V}$ , the divalent lead could be reduced to Pb in the previous cathodic scanning; On the other hand, in the subsequent positive or anodic scanning, the Pb will be oxidized to  $\text{PbSO}_4(\text{O})$  before the formation of  $\text{PbO}_2$ . However, if the initial potential is higher than  $-1.0\text{ V}$ , the  $\text{PbSO}_4(\text{R})$  from the reduction of  $\text{PbO}_2$  in the previous negative scanning will not be reduced, while only in the subsequent positive or anodic scanning the  $\text{PbSO}_4(\text{R})$  would be oxidized to  $\text{PbO}_2$ . So, through altering the initial potential of the scanning, the influence of the two types of  $\text{PbSO}_4$  on the process of the formation of  $\text{PbO}_2$  and oxygen evolution could be investigated.  $\text{PbO}_2$  can exist in two crystal forms: the rhombic ( $\alpha$ ) and the tetragonal ( $\beta$ ) ones, and  $\alpha\text{-PbO}_2$  is only formed in alkaline or neutral solutions whereas  $\beta\text{-PbO}_2$  is formed in acidic solutions [17,18], as suggested by Codaro and Vilche [19] in the following reaction sequence:



The validity of above reaction scheme has been demonstrated in Fig. 1 from the curves of voltammograms in different potential ranges, where all the curves were identified from the fifth circle of the cyclic voltammograms, and the high potential of all the scanning was kept constant at  $2.0\text{ V}$ .

The cyclic voltammograms of Pb in 4 M  $\text{H}_2\text{SO}_4$  solution in different potential ranges: (a) the potential range from  $-2.0$  to  $2.0\text{ V}$ ;

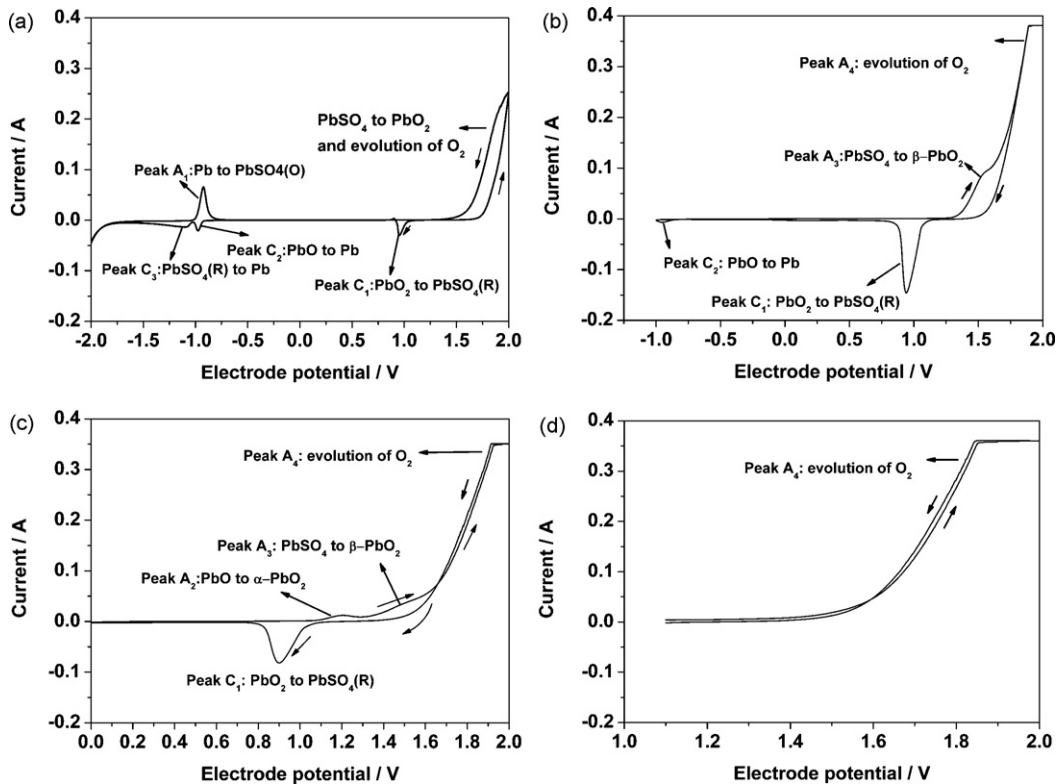


Fig. 1. The changes of the shapes of the peaks corresponding to the formation of  $\text{PbO}_2$  and oxygen evolution as a function of the scanning potential ranges.

(b) the potential range from  $-1.0$  to  $2.0$  V; (c) the potential range from  $0.0$  to  $2.0$  V; (d) the potential range from  $1.1$  to  $2.0$  V.

It was observed that as the initial potential increased, the critical potential at which the formation of  $\text{PbO}_2$  occurs, decreased from about  $1.7$  V in Fig. 1(a) to about  $1.1$  V in Fig. 1(c). Also, when the initial potential was above  $-1.0$  V (see Fig. 1(b) and (c)), the current of peak  $C_1$  increased significantly, and the current of oxygen evolution could reach  $0.35$  A. When the initial potential was increased to  $1.1$  V, no more anodic or cathodic peaks were observed except for that of oxygen evolution (see Fig. 1(d)). These features depict that the shape of anodic peaks with respect to the formation of  $\text{PbO}_2$  and oxygen evolution are related to the types of  $\text{PbSO}_4$ , and the  $\text{PbSO}_4(\text{R})$  has a higher reaction activity.

Starting from an initial potential of  $-2.0$  V (Fig. 1(a)), it was observed in each cathodic scanning, the surface layer can be reduced to Pb (peak  $C_3$ ) and subsequently, in the anodic scanning, the Pb was oxidized to  $\text{PbSO}_4(\text{O})$  (peak  $A_1$ ). Due to the low oxidation activity of  $\text{PbSO}_4(\text{O})$ , the anodic peaks  $A_2$  and  $A_3$ , which are the symbols of the formation of  $\text{PbO}_2$ , would appear at a more positive potential, which overlaps with the anodic peak of oxygen evolution. Due to the difficulty of the oxidation of  $\text{PbSO}_4(\text{O})$ , only a little  $\text{PbO}_2$  was formed, so the peak  $C_1$  which indicates the conversion from  $\text{PbO}_2$  to  $\text{PbSO}_4(\text{R})$  was low.

On the contrary, when the initial potential was started from  $-1.0$  V,  $\text{PbSO}_4(\text{R})$  was not found to be reduced in the cathodic scanning, but PbO was found to be reduced to Pb as shown by peak  $C_2$  (see Fig. 1(b)). In the subsequent anodic scanning, peak  $A_1$  indicating the oxidation of Pb disappeared, which may be attributed to the inert property of the surface layer formed over the Pb electrode. Because, the reduction of PbO to metallic phase Pb occurs between the outer  $\text{PbSO}_4$  layer and the inner PbO layer as reported by Rocca et al. [20]. Therefore, the intermediate Pb layer would not be oxidized in the subsequent anodic scanning due to the hindering of the outer  $\text{PbSO}_4$  layer. Therefore, no  $\text{PbSO}_4(\text{O})$  was

generated although the PbO was reduced, which means the oxidation of  $\text{PbSO}_4(\text{R})$  was easier, and the quantity of  $\text{PbO}_2$  was large. Therefore the cathodic peak  $C_1$  which indicates the conversion from  $\text{PbO}_2$  to  $\text{PbSO}_4(\text{R})$  was higher. As the  $\text{PbO}_2$  is the catalyzer of the reaction of oxygen evolution [19], the quantity of oxygen was also greater.

Moreover, when starting from an initial potential of  $0.0$  V, both the PbO and  $\text{PbSO}_4$  were not observed to be reduced in the cathodic scanning, so the surface of the electrode was still  $\text{PbSO}_4(\text{R})$  before the formation of  $\text{PbO}_2$ , which would be oxidized easily. Therefore, the peak  $A_2$  attributed to the oxidation of PbO to  $\alpha\text{-PbO}_2$  as indicated by Eq. (4) and the peak  $A_3$  attributed to the oxidation of  $\text{PbSO}_4$  to  $\beta\text{-PbO}_2$  as indicated by Eq. (5) appeared before oxygen evolution. According to Pavlov et al. [15,16,21], PbO is formed in the potential range  $-0.4$  to  $0.9$  V, where the surface layer of lead electrode is covered with a compact  $\text{PbSO}_4$  layer but is permeable to  $\text{H}^+$  and  $\text{OH}^-$  ions while impermeable to  $\text{Pb}^{2+}$  and  $\text{SO}_4^{2-}$  ions. In the presence of an electric field, the  $\text{OH}^-$  ions can migrate towards the inner layer easily [15,22,23], and specifically when the potential is positive than  $-0.4$  V, the concentration of  $\text{OH}^-$  ions will be high enough to form PbO, and hence the PbO could be oxidized to  $\alpha\text{-PbO}_2$  in the anodic scanning shown by peak  $A_2$ . In the case of the initial potential of  $-1.0$  V, the scanning also passed through the potential range forming PbO, but the disappearance of peak  $A_2$  (PbO to  $\alpha\text{-PbO}_2$ ) may be attributed to its positive migration, overlapping with peak  $A_3$ . However, when the initial potential was increased to  $1.1$  V, no  $\text{PbO}_2$  could be reduced to  $\text{PbSO}_4$  in the cathodic scanning, and as a result, the anodic peak due to the oxidation of  $\text{PbSO}_4$  was not observed.

It could be concluded here that, when the initial potential is lower than  $-1.0$  V, the surface layer prior to the formation of  $\text{PbO}_2$  should be  $\text{PbSO}_4(\text{O})$ , which has a low reaction activity and could be oxidized difficultly. On the contrary, when the initial potential is above  $-1.0$  V, the surface layer prior to the oxidation of  $\text{PbSO}_4$

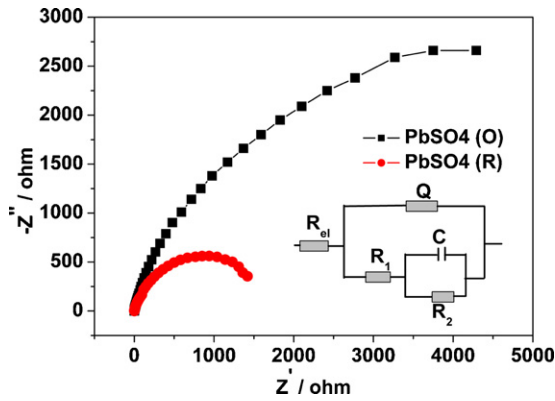


**Fig. 2.** Nyquist plots for Pb electrode in 4M H<sub>2</sub>SO<sub>4</sub>. (■) Electrode polarized at  $-2$  V for 600 s and then stepped to  $-0.95$  V for 3600 s. (●) Electrode polarized at 2 V for 600 s then stepped to 0.96 V for 3600 s.

should be PbSO<sub>4</sub>(R) which has a high reaction activity and could be oxidized easily.

### 3.2. Characterizations of PbSO<sub>4</sub>(R) and PbSO<sub>4</sub>(O)

Through EIS, SEM and XRD analyzes, two types of PbSO<sub>4</sub>, PbSO<sub>4</sub>(R) and PbSO<sub>4</sub>(O), were identified. First, the Nyquist impedance plots of the lead electrodes polarized in 4M H<sub>2</sub>SO<sub>4</sub> in different conditions were shown in Fig. 2. An equivalent circuit in EIS shown in the lower right corner of Fig. 2, could be used to fit the impedance data and the fitting results are shown in Table 1.

In Fig. 2, two different profiles are given to stand for the electrode polarized; one is at  $-2$  V for 600 s and then stepped to  $-0.95$  V for 3600 s and another is at 2 V for 600 s then stepped to 0.96 V for 3600 s. Where,  $R_{el}$  stands for the resistance of the electrolyte solu-

**Table 1**

Fit parameters for Pb electrode in 4M H<sub>2</sub>SO<sub>4</sub> at different polarization condition.

Symbol	PbSO <sub>4</sub> from Pb	PbSO <sub>4</sub> from PbO <sub>2</sub>
$R_{el}$ ( $\Omega$ )	0.38	0.63
$Q$ ( $S \cdot s^n \times 10^{-5}$ )	3.68	4.02
$n$	0.60	0.58
$R_1$ ( $\Omega$ )	0.38	0.31
$C$ ( $\mu F$ )	3.28	4.03
$R_2$ ( $\Omega$ )	9629	1770

tion,  $Q$  for the constant phase element which is decided by the value of  $n$ . If  $0 \leq n < 0.5$ ,  $Q$  represents resistance, and if  $0.5 \leq n < 1$ ,  $Q$  represents the double layer capacitance [24].  $R_1$  denotes the resistance of electrochemical reaction;  $C$  is the absorption capacitance;  $R_2$  is the ions transferring resistance through the PbSO<sub>4</sub> layer. From Table 1, the values of  $R_2$  vary substantially, which means ion-transfer resistances of the two PbSO<sub>4</sub> deposits have a big difference. Generally, the growth of PbO<sub>2</sub> crystal depends on the rate of ion-transfer [19], so PbSO<sub>4</sub>(R) can be oxidized to PbO<sub>2</sub> much easier than PbSO<sub>4</sub>(O). Therefore, the significant difference of the curves shapes in Fig. 1 is reasonable.

The SEM scanning results of PbSO<sub>4</sub>(O) and PbSO<sub>4</sub>(R) layers formed on the Pb electrode are displayed respectively in Fig. 3(b) and (d). It shows the crystal size of PbSO<sub>4</sub>(O) is smaller than that of PbSO<sub>4</sub>(R), and gives a denser structure than the latter one. Besides, the specific surface area of the PbSO<sub>4</sub>(O) is also smaller. Although the two types of PbSO<sub>4</sub> were prepared from the same material pure Pb (see Fig. 3(a)), the high specific surface area of the PbO<sub>2</sub> (Fig. 3(c)) was the real reason for the high specific surface area of PbSO<sub>4</sub>(R).

Further identification of the phase composition of two samples of PbSO<sub>4</sub>(O) and PbSO<sub>4</sub>(R) was performed through the X-ray diffraction as shown in Fig. 4. In general, PbSO<sub>4</sub> is existing in two forms: cubic and orthorhombic. However, the cubic form is rarely reported in the literature. The XRD pattern of the two types of PbSO<sub>4</sub>

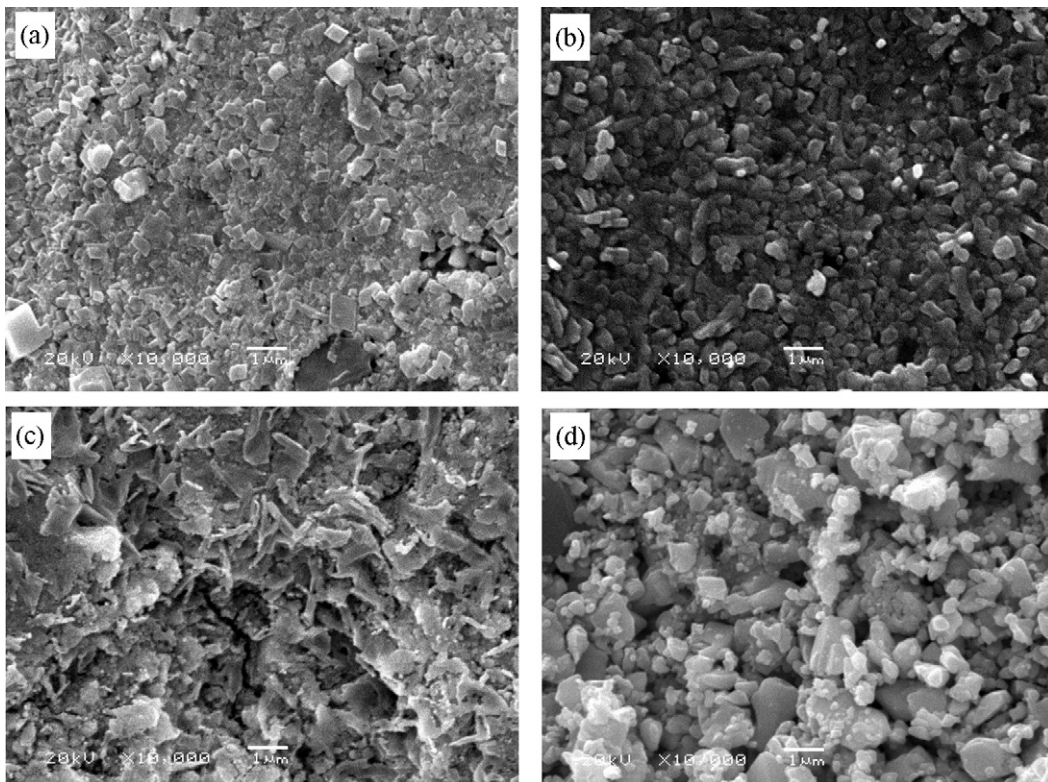


**Fig. 3.** SEM images of the surface layer of the Pb electrode. (a) Pb, prepolarized at  $-2$  V for 600 s; (b) PbSO<sub>4</sub>(O), prepared from the oxidation of Pb at  $-0.95$  V for 3600 s; (c) PbO<sub>2</sub>, prepared from Pb polarized at 2 V for 600 s; (d) PbSO<sub>4</sub>(R), prepared from the reduction of PbO<sub>2</sub> at 0.96 V for 3600 s.

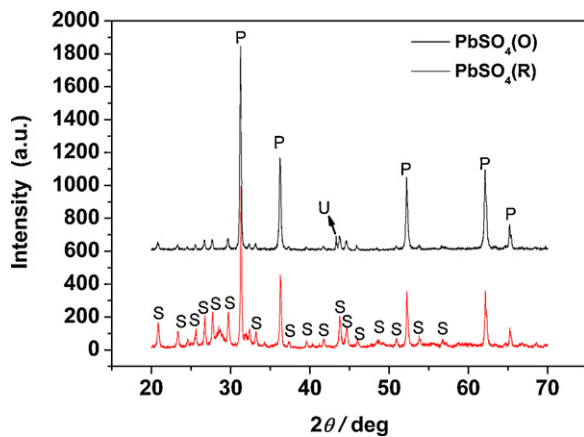


**Fig. 4.** XRD pattern of the two samples of  $\text{PbSO}_4(\text{O})$  (the upper) and  $\text{PbSO}_4(\text{R})$  (the lower): P stands for Pb; S stands for orthorhombic  $\text{PbSO}_4$ ; U stands for unexpected peak.

is shown in Fig. 4. Because the sample was scraped off from the Pb electrode, the characteristic peaks of metallic phase Pb were manifested clearly. The rest of diffraction peaks of the two samples are observed in agreement with JCPDS data of orthorhombic  $\text{PbSO}_4$  (JCPDS #: 36-1461), except for the peak “U” at the angle of  $43.3^\circ$ . Only the peak “U” in the upper pattern is in agreement with JCPDS data of cubic  $\text{PbSO}_4$  (JCPDS #: 45-0839). Since the characteristic peaks of  $\text{PbSO}_4(\text{O})$  are in good agreement with JCPDS data of orthorhombic form but have a relatively large discrepancy with JCPDS data of cubic form, it is suggested that  $\text{PbSO}_4(\text{O})$  should belong to the orthorhombic form. Therefore, the two types of  $\text{PbSO}_4$  are of the same crystal form, and the significant difference in reaction activity should not be attributed to the different crystal forms of  $\text{PbSO}_4$ .

### 3.3. Battery restoring performance

Through inverse charging, as illustrated through Eqs. (1)–(3), the active material on the negative electrode could be transformed from  $\text{PbSO}_4(\text{O})$  to  $\text{PbSO}_4(\text{R})$ , and thus reactivated. As shown in Table 2, the initial capacity ( $C_i$ ) before recovering was about 0.93 Ah and the discharging time was 3357 s. While, the capacity after inverse charging ( $C_r$ ) was 2.15 Ah and the discharging time reached 7725 s. Therefore, the new capacity after inverse charging increased significantly, which was more than twice of the initial value. Fig. 5 shows the discharge curves of the battery before and after inverse charging. It is observed that the voltage of the sulfated battery dropped sharply after 2.0 V, but the voltage of the recovered battery dropped slowly until 1.9 V, which means the discharging capability of the recovered battery has been increased. The new capacity could not reach the full capacity of about 4 Ah, which may be due to other failure modes. However, this could be solved by refreshing the electrolyte with a concentrated sulfuric acid, as reported by Karami et al. [11,12], who found that the capacity of a discarded battery could be recovered to more than 80% of a fresh and non-sulfated one by replacing with a new  $\text{H}_2\text{SO}_4$  solution of  $1.28 \text{ g cm}^{-3}$ . However, after the battery was recharged, the density of the electrolyte could increase to be much higher than  $1.28 \text{ g cm}^{-3}$ , which is detrimental to the battery according to Pavlov et al. [25,26].

**Table 2**

Discharge capacities of the battery before and after inversely charging (4-h rate).

Battery	The discharging time, $t$ (s)	The capacity, $C$ (Ah)
The sulfated battery	3357	0.93
The recovered battery	7725	2.15

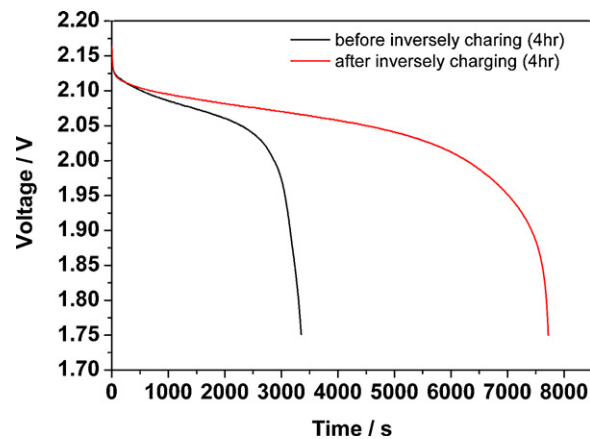


**Fig. 5.** Discharge curves of a fully sulfated lead-acid battery (2V/4Ah) at 4-h rate before inverse charging and after inverse charging.

## 4. Conclusions

Two different types of  $\text{PbSO}_4$  have been identified and their different reaction activity enables them to be used in battery capacity recovery through a suggested reaction scheme as illustrated by the authors.

In the CV tests, the process of the oxidation of  $\text{PbSO}_4$  to  $\text{PbO}_2$  was investigated. It was observed that  $\text{PbSO}_4(\text{O})$  could be oxidized difficultly, but  $\text{PbSO}_4(\text{R})$  could be oxidized easily. Through SEM and EIS analyzes,  $\text{PbSO}_4(\text{O})$  was found with a small crystal grain size, a dense structure, and a high ion-transfer resistance; on the contrary,  $\text{PbSO}_4(\text{R})$  was found with a little big crystal grain size, a loose structure, and a low ion-transfer resistance, which means the reaction activity of  $\text{PbSO}_4(\text{R})$  is much greater than that of  $\text{PbSO}_4(\text{O})$ . But the XRD results showed that the two types of  $\text{PbSO}_4$  belong to the orthorhombic  $\text{PbSO}_4$ , which suggests that the significant difference in reaction activity of the two types of  $\text{PbSO}_4$  should not be attributed to the different crystal forms of  $\text{PbSO}_4$ . The different reaction activity of  $\text{PbSO}_4(\text{O})$  and  $\text{PbSO}_4(\text{R})$  was applied in inverse charging to reactivate the sulfated negative electrode, and the result showed that the new capacity after inverse charging was more than twice of the initial value. The discovery of the different reaction activity of the two types of  $\text{PbSO}_4$  provides the mechanism for the methods of the inverse charging or repeating redox process at positive potential ranges to reactivating sulfated negative electrode, and can also bring other novel recovering method, which means as long as  $\text{PbSO}_4(\text{O})$  is transformed to  $\text{PbSO}_4(\text{R})$ , the sulfated negative electrode could be reactivated.

## References

- [1] F. Mattera, D. Bencheitrite, D. Desmettre, J.L. Martin, E. Potteau, J. Power Sources 116 (2003) 248–256.
- [2] H.A. Catherino, F.F. Feres, F. Trinidad, J. Power Sources 129 (2004) 113–120.
- [3] W. Kappus, A. Winsel, J. Power Sources 8 (1982) 159–173.
- [4] K. Sawai, T. Funato, M. Watanabe, H. Wada, K. Nakamura, M. Shiomi, S. Osumi, J. Power Sources 158 (2006) 1084–1090.
- [5] M. Shiomi, T. Funato, K. Nakamura, K. Takahashi, M. Tsubota, J. Power Sources 64 (1997) 147–152.
- [6] K. Nakamura, M. Shiomi, K. Takahashi, M. Tsubota, J. Power Sources 59 (1996) 153–157.
- [7] P.T. Moseley, R.F. Nelson, A.F. Hollenkamp, J. Power Sources 157 (2006) 3–10.
- [8] A.W. Stienecker, T. Stuart, C. Ashtiani, J. Power Sources 156 (2006) 755–762.
- [9] A. Kirchev, F. Mattera, E. Lemaire, K. Dong, J. Power Sources 191 (2009) 82–90.
- [10] R.F. Nelson, E.D. Sexton, J.B. Olson, M. Keyser, A. Pesaran, J. Power Sources 88 (2000) 44–52.
- [11] H. Karami, R. Asadi, J. Power Sources 191 (2009) 165–175.
- [12] H. Karami, B. Masoomi, R. Asadi, Energy Convers. Manage. 50 (2009) 893–898.
- [13] Y. Yamamoto, M. Matsuoka, M. Kimoto, M. Uemura, C. Iwakura, Electrochem. Acta 41 (1996) 439–444.

- [14] Y. Yamamoto, K. Fumino, T. Ueda, M. Nambu, *Electrochem. Acta* 37 (1992) 199–203.
- [15] D. Pavlov, *J. Electrochem. Soc.* 117 (1970) 1103–1109.
- [16] Y. Guo, *J. Electrochem. Soc.* 138 (1991) 1222–1227.
- [17] D. Devilliers, M.T. Dinh Thi, E. Mah, V. Dauriac, N. Lequeux, *J. Electroanal. Chem.* 573 (2004) 227–239.
- [18] I. Ivanov, Y. Stefanov, Z. Noncheva, M. Petrova, T. Dobrev, L. Mirkova, R. Vermeersch, J.P. Demaerel, *Hydrometallurgy* 57 (2000) 125–139.
- [19] E.N. Codaro, J.R. Vilche, *Electrochem. Acta* 42 (1997) 549–555.
- [20] E. Rocca, J. Steinmetz, S. Weber, *J. Electrochem. Soc.* 146 (1999) 54–58.
- [21] D. Pavlov, *J. Electrochem. Soc.* 116 (1969) 316–319.
- [22] P. Ruetschi, *J. Electrochem. Soc.* 120 (1973) 331–336.
- [23] Y. Guo, *J. Electroanal. Chem.* 317 (1991) 229–241.
- [24] C.-S. Dai, B. Zhang, D.-L. Wang, T.-f. Yi, X.-G. Hu, *J. Alloys Compd.* 422 (2006) 332–337.
- [25] D. Pavlov, A. Kirchev, M. Stoycheva, B. Monahov, *J. Power Sources* 137 (2004) 288–308.
- [26] D. Pavlov, G. Petkova, T. Rogachev, *J. Power Sources* 175 (2008) 586–594.